Weierstrass Institute for
Applied Analysis and Stochastics

DFG-Forschungszentrum MATHEON
Mathematik für Schlüsseltechnologien

Statistical issues in accessing brain functionality and anatomy

Jörg Polzehl and Karsten Tabelow

UseR! 2010, Kaleidoscope I, July 22

- Strong magnetic field (usually $1.5-3$ Tesla(T), up to 10.5 T)
- Radio frequency pulse at Lamour-frequency
- Measuring relaxation times (T_1 (z-direction), T_2 (phase coherence in x-y), and $T_2^\star$) of magnetic spin excitation in receiver coil(s)
- Image generation by 2D-FFT

Goal: Understanding how the brain works

functional Magnetic Resonance Imaging (fMRI):

- Locate brain functionality in grey matter
- Assessment of population variability
- Identification of functional networks
- Presurgical planning and diagnosis

Diffusion weighted MR imaging (DWI):

- Focus on white matter anatomy
- Measure anisotropy of water diffusion in the brain using additional magnetic field gradients
- Restricted water diffusion within neuronal fiber bundles

fMRI experiments and data

- 3D x T data
- $64 \times 64 \times 30$ voxel
- Resolution $2 \times 2 \times 4mm^3$
- image formats: DICOM / AFNI / NIFTI / Analyze
- noise: termal noise, system noise (variations in magnetic field, magnetic field inhomogeneity), physiological noise (respiration, heart beat)
- artifacts from head motion
- spatial and temporal correlation

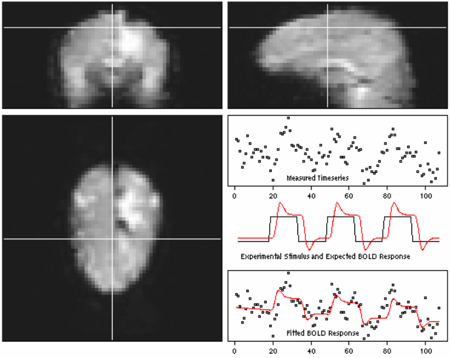

Tools in R (Medical imaging taskview):

- Analysis: Packages fMRI and AnalyzefMRI
- data IO: Packages fmri, oro.dicom, tractor.base

Modeling fMRI data (General linear model approach)

- Observed Signal in voxel i:

$$\begin{aligned} Y_{it} &= \int_0^\infty h(t-t')s(t')dt' + g(i,t) + \varepsilon_{it} \qquad t = 1,\dots,T \qquad i = (i_x, i_y, i_z) \\ &= x_t^\top \beta_i + \varepsilon_{it} \qquad x_t = (\int_0^\infty h(t-t')s(t')dt', 1, t, t^2, g_1(t), \dots)^\top \end{aligned}$$

- Prewhitening using $AR(1)$ error model
- Estimate parameters by least squares
- Contrast: $\gamma = c^\top \beta, \quad \hat{\gamma}_i = c^\top \hat{\beta}_i, \quad \mathbf{D}\hat{\gamma}_i = c^\top \mathbf{D}\hat{\beta}_i c.$
- Statistical parametric map (SPM): $\Gamma = (\hat{\gamma}_i), \quad i = (i_x, i_y, i_z)$
- Inference based on SPM

```
library(fmri)
data128moto  <- read.AFNI("test2_128_motor_re+orig")
hrf <- fmri.stimulus(scans = 105, c(18, 48, 78), 15, 2)
z <- fmri.design(hrf)
spm128moto <- fmri.lm(data128moto,z,keep="all")
pvalue128moto <- fmri.pvalue(spm128moto)
plot(pvalue128moto,maxpvalue=0.01,file="test2_128_motor",device="png")‘
```

Smoothing in fMRI

Voxelwise analysis

- Multiple testing 100000 - 500000 voxel
- Adjustment by Bonferroni or FDR leads to high thresholds

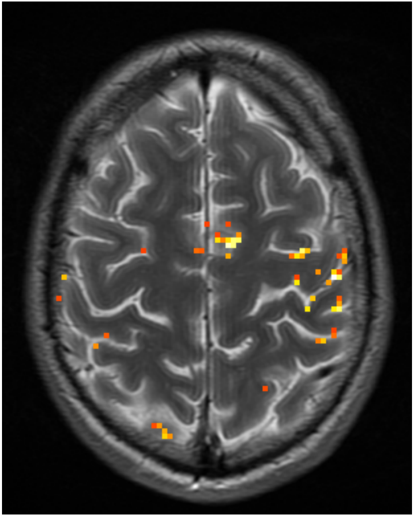

voxelwise decision

Smoothing in fMRI

Gaussian filter (FWHM bandwidth) + RFT

- Multiple testing 100000 - 500000 voxel
- Spatial smoothing increases SNR and decreases number of independent tests
- threshold selection by Random Field Theory

Code:

```
spm128motosm6 <- fmri.smooth(
        spm128moto,hmax=6,
        adaptive=FALSE)
pv128motosm6 <- fmri.pvalue(
         spm128motosm6)
plot(pv128motosm6,maxpvalue=0.01,
         file="test2_128_motorsm6",
        device="png")‘
```

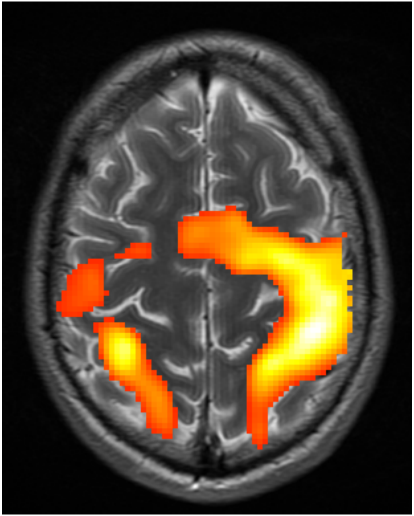

decision using nonadaptive smoothing

Gaussian filter (FWHM bandwidth) + RFT

- Increase of resolution decreases SNR
- Use of standard filters loses gain from higher spatial resolution due to larger bandwidths

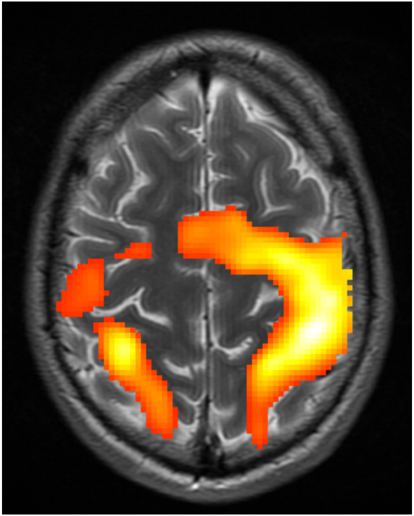

Non-adaptive smoothing + RFT

Adaptive smoothing (AWS) + RFT

- Increase of resolution decreases SNR
- Use of standard filters loses gain from higher spatial resolution due to larger bandwidths
- Use of adaptive smoothing preserves spatial structure

Code:

```
spm128motoaws6 <- fmri.smooth(
        spm128moto,hmax=6)
pv128motoaws6 <- fmri.pvalue(
        spm128motoaws6)
plot(pv128motoaws6,maxpvalue=0.01,
        file="test2_128_motoraws6",
        device="png")‘
```

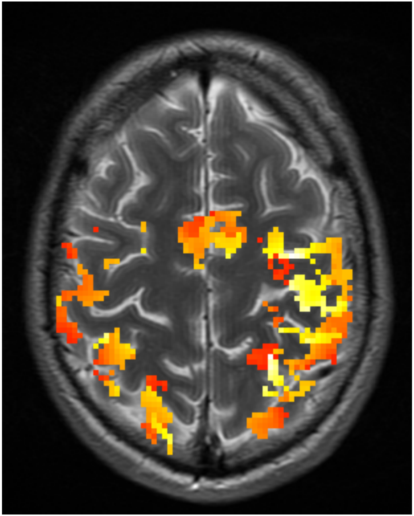

Structural adaptive smoothing + RFT

Increasing resolution: going adaptive

Adaptive segmentation

- Increase of resolution decreases SNR
- Use of standard filters loses gain from higher spatial resolution due to larger bandwidths
- Use of adaptive smoothing preserves spatial structure

Code:

```
spm128motosegm6 <- fmri.segment(
        spm128moto,hmax=6)
plot(pv128motosegm6,
        file="test2_128_motorsegm6",
        device="png")‘
```

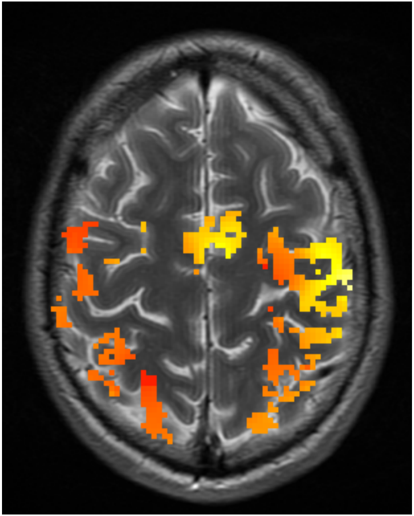

Structural adaptive segmentation

- 3D + S^2 data
- Measurements of integral values on a regular grid of voxel (size $\approx 1mm^3$)
- Structures of interest have a diameter of $10-30\mu m$ and length of up to $10cm$
- $1-30$ measurements without gradient field (S_0)
- $12-180$ measurements with additional gradient ($S(\vec{g})$)
- gradient directions uniformly sampled from the sphere S^2
- Observations live in an 3D orientation score $R^3 \rtimes S^2$.

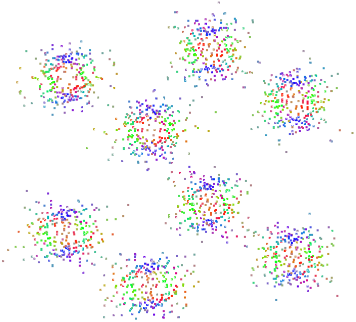

ADC $-log(S_{\vec{g}}/S_0)$, 140 gradients in one voxel

Tools in R (Medical imaging taskview):

- Analysis: Package dti and TractoR project

Code:

```
library(dti); demo(mixtens_art) # dwi data in object z
show3d(z[5:6,5:6,5:6],FOV=1); rgl.bg(color="white") # Visualize observations
```

The tensor model

- Diffusion characterized by a symmetric positive semi-definite 3×3 matrix $\mathscr{D}$
- Nonlinear Model

$$S_i(\vec{g}) \sim Rice(\theta_i \exp(-b\vec{g}^\top \mathscr{D}_i \vec{g}), \sigma_i^2)$$

- Nonlinear regression with positivity constraints

$$\begin{aligned}
\mathbf{R}(\zeta, \theta, \mathscr{D}) &= \sum_j \frac{(\zeta(\vec{g}_j) - \theta \exp(-b\vec{g}_j^\top \mathscr{D}_i \vec{g}_j))^2}{\sigma_{j,i}^2} \\
\begin{pmatrix} \hat{\theta}_i \\ \hat{\mathscr{D}}_i \end{pmatrix} &= \arg\min_{\theta, \mathscr{D}} \mathbf{R}(\hat{\zeta}_i, \theta, \mathscr{D})
\end{aligned}$$

Code:

```
library(dti)
bvec <- read.table("b-directions.txt") # gradients
dwobj <- readDWIdata(bvec,"s0004",format="DICOM",xind=48:204,yind=19:234,nslice=66)
dwobj <- sdpar(dwobj,level=300)# variance estimates and threshold
nytens <- dtiTensor(dwobj) # tensor estimates
```

Tensor characteristics

- Mean diffusivity $Tr(\mathscr{D}) = \mu_1 + \mu_2 + \mu_3$
- Fractional anisotropy (FA)

$$FA = \sqrt{\frac{3}{2}}\sqrt{\frac{(\mu_1 - \langle\mu\rangle)^2 + (\mu_2 - \langle\mu\rangle)^2 + (\mu_3 - \langle\mu\rangle)^2}{\mu_1^2 + \mu_2^2 + \mu_3^2}},$$

- Geodesic anisotropy (GA) (Fletcher (2004), Corouge (2006))

$$GA = (\sum_{i=1}^{3}(log(\mu_i) - \overline{log(\mu)})^2)^{1/2}, \quad \overline{log(\mu)} = \frac{1}{3}\sum_{i=1}^{3} log(\mu_i)$$

- Bary-coordinates (characterizing spherical, planar and linear shape)

$$C_s = \frac{\mu_3}{\langle\mu\rangle} \quad C_p = \frac{2(\mu_2 - \mu_3)}{3\langle\mu\rangle} \quad C_l = \frac{(\mu_1 - \mu_2)}{3\langle\mu\rangle}$$

Code:

```
nytenschar <- extract(nytens,c("fa","ga","md",''evalues",''andir"))
nydtind <- dtiIndices(nytens)
```

- Gray-valued map of mean diffusivity
- Color coded FA / GA maps
  - Principal eigenvector
    $\vec{e}_1 = (e_{1x}, e_{1y}, e_{1z})$ color coded in RGB
  - Commonly used
    $$(R,G,B) = (|e_{1x}|, |e_{1y}|, |e_{1z}|) \cdot FA$$
  - Better alternative
    $$(R,G,B) = (e_{1x}^2, e_{1y}^2, e_{1z}^2) \cdot FA$$

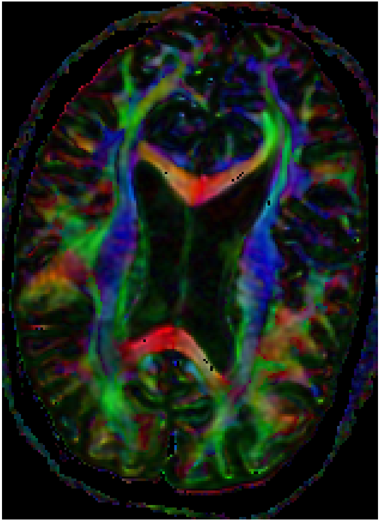

Code:

```
nyccfa35 <- plot(nydtind,slice=35)
write.image(nyccfa35,"nyccfa35.png")
```

Smoothing in DWI ?

- Adaptive smoothing provides more stable estimates without loss of structure
- enables to reduce recording time

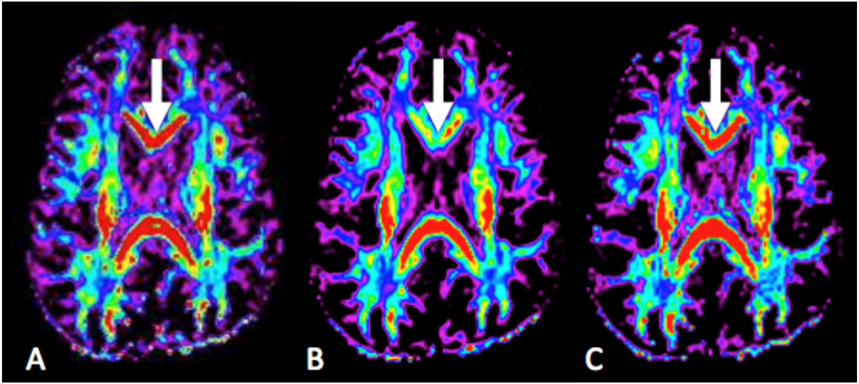

A: unsmoothed B: non-adaptive C: adaptive

Limitations of Diffusion Tensor Imaging

- DT-model assumes homogeneous fiber structure in a voxel
- Reality: high percentage of voxel with fiber crossings or bifurcations

More accurate description

- $P(\vec{r},\vec{r}',\tau)$ probability for a particle to diffuse from position $\vec{r}'$ to $\vec{r}$ in time τ
- Mean diffusion function (over a voxel V):

$$P(\vec{R},\tau) = \int_{\vec{r}'\in V,\ \vec{R}=\vec{r}-\vec{r}'} P(\vec{r},\vec{r}',\tau)p(\vec{r}')d\vec{r}'$$

- Orientation density function (ODF) (weighted radial projection of P, Aganji 2009)

$$\psi_{(w)}(\vec{u},\tau) = \int_0^\infty r^2 P(r\vec{u},\tau)dr = \frac{1}{4\pi} - \frac{1}{8\pi^2}\int_0^{2\pi} {}_{\theta=\pi/2} \bigtriangledown_b^2 ln(-lnE))d\phi$$

for anisotropic Gaussian diffusion using Funk-Radon transform, $E(\vec{q}) = \mathrm{E} S_{\vec{q}}/S_0$, $\vec{q} = q\vec{u}$ represented as (q,θ,ϕ) and $\bigtriangledown_b^2 E = \frac{1}{q^2}\left[\frac{1}{\sin(\phi)}\frac{\delta}{\delta\theta}(\sin\theta\frac{\delta E}{\delta\theta}) + \frac{1}{\sin^2\theta}\frac{\delta^2 E}{\delta\phi^2}\right]$

Q-Ball imaging:

- expansion into spherical harmonics (Descoteaux et al., (2007), Aganj (2009))

$$\ln(-\ln E(\vec{g}_i)) = \sum_{j=1}^{J} c_j Y_j(\vec{g}_i) \quad \psi_w(\vec{u}) = \frac{1}{2\sqrt{\pi}} Y_1(\vec{u}) - \frac{1}{16\pi^2} \sum_{j=2}^{J} 2\pi P_{k_j}(0) k_j (k_j+1) c_j Y_j(\vec{u})$$

- Fast (linear), high-frequency artifacts (needs regularization), ODF via Funk-Radon transform is non-linear in E ... ($ln(-lnE)$)).

Tensor Mixture Models:

- Model:

$$\frac{S(\vec{g})}{S_0} = \sum_i w_i \exp(-b\vec{g}^\top \mathscr{D}_i^{-1} \vec{g}) \quad \sum_i w_i = 1, \quad w_i \geq 0$$

- ODF: Mixture of Angular Central Gaussian distributions

$$\psi(\vec{u}, \tau) = (4\pi)^{-1} \sum_i w_i |\mathscr{D}_i|^{-1/2} (\vec{u}^\top \mathscr{D}_i^{-1} \vec{u})^{-3/2}$$

- parameter identifiability ? to flexible ... Reparametrization:

$$\mathscr{D}_i = \lambda_2 I_3 + (\lambda_1 - \lambda_2) d_i d_i^\top$$

Q-Ball

```
zqball <- dwiQball(z,order=8,
                   lambda=1e-2)
show3d(zqball, FOV=1)
rgl.bg(color="white")
```

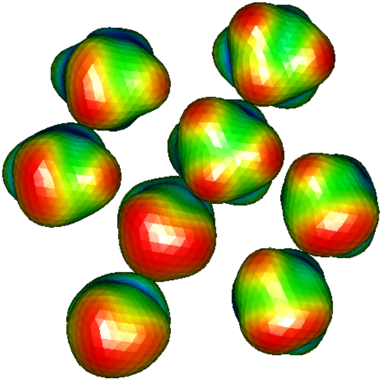

Tensor-Mixtures

```
zmix5 <- dwiMixtensor(z,maxcomp=5)
show3d(zmix5, FOV=1)
rgl.bg(color="white")
```

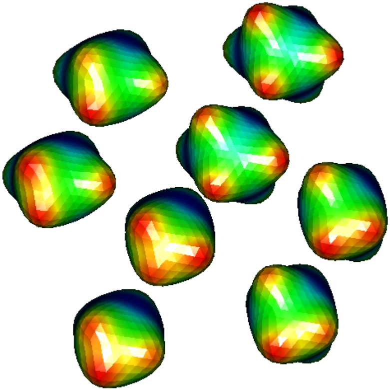

- DTI and tensor mixture models provide vector fields of preferred directions
- Currently implemented: Streamline tracking for tensor and tensor mixture models
- Alternatives: probabilistic tracking, minimization of energy functionals

Code:

```
nymix4 <- tracking(dwobj,maxcomp=4)
tracks <- tracking(nymix4,roiz=40)
show3d(tracks, FOV=1)
rgl.bg(color="white")
```

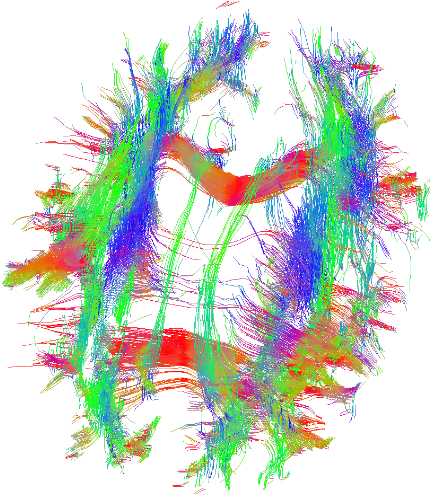

Fiber tracks crossing slice 35 using tensor mixtures order 4

Open problems: Connectivity

Combine results from

- fMRI (identification of regions with specific functionality)
- DWI (identification of fiber bundel connections)

Goals (see e.g. Hagmann et.al. PLOSone (2007)), Pittsburgh Brain competition.

- Construction of connectivity maps
- weighted networks of brain connections (500-4000 nodes, 25000 - 100000 edges)

Collaborations

Joint Work with:

- Henning Voss, Weill Medical College, Cornell University

Cooperation:

- Citigroup Biomedical Imaging Center, Weill Medical College, Cornell University
- University of Münster
- BNIC, Charitè, Berlin
- Max-Plank Institute for Human Cognitive and Brain Sciences, Leipzig

R-Community:

- CRAN Task View: Medical Image Analysis
  Jonathan Clayden, Pierre Lafaye de Micheaux, Volker Schmid, Brandon Whitcher

Acknowledgments:

- We thank the Weill Medical College, Cornell University, the Max Planck Institute for Human Cognitive and Brain Sciences and University of Münster and the NIH/NCRR Center for Integrative Biomedical Computing (P41-RR12553) for providing functional and diffusion-weighted MR datasets.

Further reading: General and fMRI

N Lazar (2008).
The Statistical Analysis of Functional MRI Data.
Springer series Statistics for Biology and Health.

K Tabelow, J Polzehl, HU Voss, V Spokoiny (2008).
Analyzing fMRI experiments with structural adaptive smoothing procedures.
Neuroimage, 33(1):55–62.

K Tabelow, J Polzehl, AM Ulug, JP Dyke, LA Heier, and HU Voss (2008).
Accurate localization of functional brain activity using structure adaptive smoothing.
IEEE TMI, 27(4):531–537.

K Tabelow, V Piëch J Polzehl, HU Voss (2009).
High-resolution fMRI: Overcoming the signal-to-noise problem.
Journal of Neuroscience Methods, 178, pp. 357–365.

J Polzehl, HU Voss, K Tabelow(2010).
Structural adaptive segmentation for statistical parametric mapping .
Neuroimage, 52, pp. 515–523.

Further reading : DWI

Susumu Mori (2007).
Introduction to Diffusion Tensor Imaging
Elsevier

Tabelow, K., Polzehl, J., Spokoiny, V., Voss, H. (2008).
Diffusion tensor imaging - spatial adaptive smoothing
Neuroimage, 39:1763–1773.

Polzehl, J., Tabelow, K. (2009).
Structure adaptive smoothing Diffusion Tensor Imaging data: the R Package dti
Journal of Statistical Software, 31, 1–24.

Tabelow, K., Polzehl, J. (2010).
Expansion of the orientation distribution function in terms of the angular central Gaussian distribution.
Manuscript